Parasitology International 105 (2025) 102995

Contents lists available at ScienceDirect

Parasitology International

journal homepage: www.elsevier.com/locate/parint

Toxoplasma GRA15 expression on dendritic cells inhibits B cell differentiation and antibody production

Yuki Nakayama [a,b], Fumiaki Ihara [a,b], Daisuke Okuzaki [c,e,f], Yoshifumi Nishikawa [g], Miwa Sasai [a,b,c,d], Masahiro Yamamoto [a,b,c,d,*]

[a] Department of Immunoparasitology, Research Institute for Microbial Diseases, Osaka University, Suita, Osaka 565-0871, Japan
[b] Laboratory of Immunoparasitology, WPI Immunology Frontier Research Center, Osaka University, Suita, Osaka 565-0871, Japan
[c] Center for Infectious Disease Education and Research, Osaka University, Suita, Osaka 565-0871, Japan
[d] Center for Advances Modalities and Drug Delivery Systems, Osaka University, Suita, Osaka 565-0871, Japan
[e] Laboratory of Human Immunology (Single Cell Genomics), WPI Immunology Frontier Research Center, Osaka University, Suita, Osaka 565-0871, Japan
[f] Bioinformatics Center, Research Institute for Microbial Diseases, Osaka University, Suita, Osaka 565-0871, Japan
[g] National Research Center for Protozoan Diseases, Obihiro University of Agriculture and Veterinary Medicine, Obihiro, Hokkaido 080-8555, Japan

ARTICLE INFO

Keywords:
Toxoplasma gondii
GRA15
Specific antibody production
B cell
Plasma cell and germinal center B cell

ABSTRACT

One of the dense granule proteins named GRA15 in *Toxoplasma gondii* (*T. gondii*), is known to support an innate immune response in host through activation of NF-κB. However, little is known about advantages of GRA15 for parasites. By examining the role of GRA15 in the host-parasite interactions, it was clarified that GRA15 in *T. gondii* suppressed acquired immune responses in host. Wild-type parasite infection to C57BL/6 mice resulted in lower titers of *T. gondii* antibody and lower plasma cell counts compared to Δgra15 *T. gondii*. To identify host cells in which GRA15 acts to suppress antibody production, we generated conditional knock-in mice that express GRA15 in specific cell lineages. Anti-*T. gondii* antibodies were not reduced in macrophages of conditional knock-in mice after infection with Δgra15 *T. gondii*, while the production of *T. gondii* antibody was suppressed in dendritic cells of the conditional knock-in mice (CD11c-Cre/GRA15cKI). In the CD11c-Cre/GRA15cKI immunized with ovalbumin (OVA), the titers of anti-OVA antibody were reduced compared to control mice. Furthermore, the number of OVA antigen-specific T cells was also decreased in CD11c-Cre/GRA15cKI. These data showed that GRA15 in dendritic cells suppressed T cell-mediated humoral immunity. These findings might implicate the pathological significance of GRA15 and facilitate *Toxoplasma* vaccines production.

1. Introduction

Toxoplasma gondii is a zoonotic protozoan pathogen of the phylum Apicomplexa. It is a widespread parasite, estimated to infect more than 1/3 of the world's human population [1]. Sexual reproduction of *T. gondii* takes place exclusively in the cat intestine, but it is capable of infecting cells of all warm-blooded animals [1,2]. It is transmitted to humans by oral ingestion of tissue cysts in undercooked meat and oocysts in raw water and vegetables contaminated with cat faces [1,2].

T. gondii infects a host cell form parasitophorous vacuoles membrane inside the infected host cell and reproduces asexually. *T. gondii* secretes various virulence factors such as rhoptry proteins (ROP) and dense granule (GRA) proteins into the host cell for survival [3–5]. Many virulence factors inhibit host immunity and help the parasite to survive. For example, ROP5 and ROP18 inactivate the IFNγ-induced immunity-related GTPases that promote killing by disrupting the parasitophorous vacuole membrane [6–10]. ROP16 and *Toxoplasma* inhibitor of STAT1-dependent transcription, TgIST, inhibit IL-12 secretion and block IFN-dependent signaling [11–14].

On the other hand, the enigmatic virulence factor GRA15, expressed in type II *T. gondii*, activates host immunity. GRA15 is known to induce NF-κB activation [15–18]. NF-κB is a dimeric protein that acts as a transcription factor and is composed of five subunits: RelA, RelB, c-Rel, p50, and p52. They usually bind to IκB protein and inhibit NF-κB activity. GRA15 directly binds to TNF receptor-related factors (TRAFs), which are adapter proteins for signaling pathways of TNF receptor-1 and

* Corresponding author at: Department of Immunoparasitology, Research Institute for Microbial Diseases, Osaka University, 3-1, Yamadaoka, Suita, Osaka 565-0871, Japan.
E-mail address: myamamoto@biken.osaka-u.ac.jp (M. Yamamoto).

https://doi.org/10.1016/j.parint.2024.102995
Received 3 October 2024; Received in revised form 8 November 2024; Accepted 13 November 2024
Available online 17 November 2024

Toll-like receptors, and leads to degradation of IκB proteins [15,18–20]. As a result, the activated NF-κB complex moves into the nucleus, where transcription is induced. Activation of the NF-κB pathway by GRA15 has been demonstrated to induce the secretion of IL-12 and IFN-γ in mouse macrophages and to upregulate CD40 in human monocytes [15–17,21]. These innate immune activations appear to be a beneficial effect for the host. Recent report suggested that GRA15 may increase the motility of infected dendritic cell-like macrophages to spread infection throughout the body [22], just as GRA6 induces neutrophils [23]. However, its advantage for *T. gondii* during the infection *in vivo* remains unclear. In particular, few reports have examined the effects of the presence of GRA15 on the acquired immune system of B cells and T cells during *T. gondii* infection. Therefore, understanding how GRA15 influences the adaptive immune response is crucial, especially considering its potential application as a vaccine adjuvant. Given that GRA15 is expected to be utilized as a vaccine adjuvant due to its immunostimulatory properties [24,25], further research in this area is warranted.

Here we focused on the effects of GRA15 on B cells responses such as antibody production. We also generated transgenic mice expressing GRA15 on dendritic cells (DCs) and macrophages to assess the impact on host immunity when GRA15 is expressed on cells susceptible to *T. gondii* infection. We found that GRA15 has a novel aspect that suppresses specific antibody production when expressed on DCs.

2. Materials and methods

2.1. Mice

C57BL/6NCrSlc mice were purchased from Japan SLC, Inc. CD11c-Cre transgenic mice were provided by Dr. Hiroaki Henmi. LysM-Cre transgenic mice were provided by Dr. Shizuo Akira. All mice were maintained under specific pathogen free conditions. All experiments were performed on 6–12-week-old mice. Mouse experiments were randomized in both sexes. All animal experiments were conducted with the approval of the Animal Research Committee of Research Institute for Microbial Diseases in Osaka University.

2.2. Generation of LSL-GRA15 mice

The T7-transcribed Rosa26_gRNA1 products, which were amplified by using KOD FX NEO (Toyobo) and the primers (Rosa26_gRNA1 5′-TTAATACGACTCACT ATAGGactccagtctttctagaagaGTTTTAGAGCTAGAAATAGCAAGTTAAAAT −3′; common_R2 5′- AAAAGCACCGACTC GGTGCCACTTTTTCAAGTTGATAACG GACTAGCCTTATTTTAACTTGCTATTTCTAGCTCT 3′) were used as the subsequent generation of Rosa26_gRNA1. MEGAshortscript T7 (Life Technologies) was used for the generation of the gRNA. Cas9 mRNA was generated by *in vitro* transcription (IVT) using mMESSAGE mMACHINE T7 ULTRA kit (Life technologies) and the template that was amplified by PCR using pEF6-hCas9-Puro and the primers T7Cas9_IVT_F and Cas9_R and gel-purified as described previously [62]. The synthesized gRNA and Cas9 mRNA were purified using MEGAclear kit (Life Technologies). To generate LSL-GRA15 mice, 3.6 kb fragment containing 500 bp fragments of the intron between exon1 and exon2 of Rosa26 gene was amplified by PCR using primers (Rosa26_LA_F 5′- CCGCGGAATGGCGTGTTTTGGTTGGCGTAA −3′; Rosa26_LA_R 5′- gtcgaCTAGAAAGACTGGAGTTGCAGATCACGAG GGAAGA −3′; Rosa26_RA_F 5′- gtcgaCTAGAAGATGGGCGG GAGTCTTCTG −3′; Rosa26_RA_R 5′- ggtaccAAGCTCACAAGACCTTA GGTCAGGA −3′) and cloned in pBluescript vector. cDNA encoding the C-terminally Flag-tagged GRA15 lacking the N-terminal signal peptide was amplified using type II *T. gondii* (ME49) cDNA and the primers (GRA15_F 5′- GGATCCACCATGATTCGGTGGCTTGGGTATCTTACGGT GCTCGCTGCCGTCATTTTGCTA -3′; GRA15_R 5′- GCGGCCGCTAG CTGCT CCAATGGCTCACGGCGCGCACGCGGTCTGGGCTGCCCTTGTCG TCATCGTCTTTGTAGTCCTCGAGTGGAGTTACCGCTGATTGTGTG TCCCGTGGGCCTCCAG −3′). Splice acceptor sequence (SA) followed by the two tandem polyA signal sequences franked by loxP sequences were artificially synthesized and obtained from FASMAC. The SA-LSL sequence was ligated with the GRA15_Flag cassette. The SA-LSL-GRA15F cassette was ligated with Rosa26_LA and Rosa26_RA fragments. The resultant targeting vector was gel purified and used for injection into embryos with Rosa26_gRNA1 and Cas9 mRNA. To obtain LSL-GRA15 mice, C57BL/6 N female mice (6 wk. old) were superovulated and mated to C57BL/6 N stud males. Fertilized one-cell-stage embryos were collected from oviducts and injected into the pronuclei or the cytoplasm with 100 ng/μl Cas9 mRNA, 50 ng/μl gRNA and 50 ng/ml the targeting vector for LSL-GRA15 mice. The injected live embryos were transferred into oviducts of pseudopregnant ICR females at 0.5 day post coitus. The male pup harboring the mutation was mated to C57BL/6 N female mice and tested for the germ line transmission.

2.3. Microorganisms

T. gondii PRU strain of wild type and GRA15 knockout were created and cultured as previously described [17,26]. The parasites were maintained in Vero cells and grown with 2 % heat-inactivated fetal bovine serum (HIFBS; gibco), 50 mM 2-mercaptoethanol (2-ME; Nacalai Tesque), 100 U/ml penicillin and 0.1 mg/ml streptomycin (0.1 % PC/SM; Nacalai Tesque) supplemented with RPMI 1640 (Nacalai Tesque) in an incubator at 37 °C, 5 % CO2, and were passaged every 3 days.

2.4. Cell culture

Vero cells were maintained in an incubator at 37 °C, 5 % CO_2, with 10 % HIFBS, 50 mM 2-ME, and 0.1 % PC/SM, with the addition of RPMI 1640. Primary tail fibroblasts and Plat-E cell were maintained in an incubator at 37 °C, 5 % CO_2, with 10 % HIFBS, 50 mM 2-ME, and 0.1 % PC/SM, with the addition of DMEM (Hi-glucose) (Nacalai Tesque). Bone marrow derived macrophages were differentiated in RPMI medium containing 10 % HIFBS, 50 mM 2-ME, 0.1 % PC/SM, and 30 % L929 cell (ATCC) supernatant for 6 days, then maintained in RPMI 1640 with 5 % L929 cell supernatant under the same conditions.

2.5. Infection and treatment

Mice were intraperitoneally infected with 10^3 tachyzoites in 200 μl PBS after filtration. Artificial antigens were administered intravenously at a dose of 100 μg/mouse of OVA protein (Kanto chemical) or 5 μg/mouse of NP-AECM-Ficoll (Biosearch technologies) dissolved in PBS, and 100 μg/mouse of poly(I:C) (Sigma) was administered intraperitoneally as previously described [27,28]. A minimal quantity of blood was extracted from the orbital vein of the mice.

2.6. Measurement of specific antibody titer

For anti-*T. gondii* IgM/IgG titers, wild-type parasites were washed with PBS and then sonicated on ice for 15 min (30 s/ON and 30 s/OFF × 15 cycles, 160 W) by Bioruptor UCD-250 (Diagenode). The protocol of the Mouse IgM/IgG uncoated ELISA Kit (invitrogen) was partially modified to measure antibody titers. The parasites homogenized solution was diluted with PBS to a concentration of 10^7 parasites/ml and mixed with an equal volume of 1× coating buffer. 50 μl of the diluted solution was seeded into 96-well plates and incubated overnight at 4 °C. For anti-OVA and anti-NP-Ficoll IgM/IgG titers, OVA protein and NP-Ficoll were dissolved in coating buffer at 10 μg/ml and 5 μg/ml, respectively, and seeded into 96-well plates and incubated overnight at 4 °C. Subsequently, in accordance with the established protocol, the samples were blocked with assay buffer and incubated for one hour at room temperature with antibodies specific for HRP anti-mouse IgM and IgG. Following this incubation period, the samples were colored with TMB solution. After the incubation, the plate was read at 450 nm - 490 nm in an iMark Microplate Absorbance Reader (Bio-Rad).

2.7. Cell preparation

PECs were collected by injecting RPMI into the abdominal cavity before the mice were opened. Spleen were mashed in PBS on a 70 μm cell strainer using syringe plunger. PECs and filtrated spleen were treated with ACK and then washed with PBS.

2.8. Flow cytometry and cell soring

The cell samples (10^5–10^6 cell) were resuspended purified anti-mouse CD16/32 (Biolegend) diluted 1/200 in FACS buffer (PBS, 3 % HIFBS, 1 mM EDTA and 0.1 % NaN_3) for 5 min on ice. Antibodies cocktails were diluted 1/100, and 20 μl was added to cells for 15 min on ice. Cells were washed twice by FACS buffer. For intranuclear staining, Foxp3/Permeabilization buffer set (eBioscience) was used according to the manufacturer's instructions. For OVA tetramer staining, H-$2K^b$ OVA tetramer-SIINFEKL-PE (NIH) was added after Fc blocking at RT for 20 min. Alexa647 anti-mouse CD8 (clone: KT15; MBL), Alexa488 anti-mouse CD45.2 (Biolegend), and 7AAD (BD) were then stained at 4 °C for 20 min. Flow cytometry and cell sorting were performed using an Attune NxT flow cytometer (Thermo Scientific) and FACS Aria III (BD), respectively.

2.9. Transfection of primary tail fibroblast with retroviral vectors

The induction of primary tail fibroblasts was conducted as previously described [23]. The preparation of retroviral vectors and their subsequent transfection were conducted in accordance with the methodologies outlined in two existing papers [23,29]. Briefly, the Cre fragment or mock were cloned into pMRX-puro retroviral vector. The plasmid DNA diluted in Opti-MEM (gibco) and its 5-fold liquid volume of PEI-Max (polysciences) were seeded into Plat-E cells. 24 h following transfection, the medium was replaced, and the cells were cultivated for an additional 48 h. The virus-containing supernatants from the Plat-E cells were harvested and immediately utilized with polybrene (Nakalai Tesque) for infection. 6 h following transduction, the medium was replaced. On the next day, cells were selected by the addition of 2 μg/ml puromycin (Invivogen) to the culture medium.

2.10. Western blotting

Cells were lysed for 10 min on ice in lysis buffer (1 % NP-40, 150 mM NaCl, 20 mM Tris-HCl, pH 7.5) containing protease inhibitor cocktail (Nakalai Tesque). The supernatant of the lysate was mixed with sample buffer containing 2-ME and heat-treated at 98 °C for 3 min. The cell lysates were separated by SDS-PAGE and transferred to Immobilon-P membranes (Millipore). The membranes were blocked in 5 % skim milk in 0.02 % Tween-20 in PBS (PBS-T) for 1 h at RT, followed by incubation with primary antibodies overnight at 4 °C. Membranes were washed with 0.02 % PBS-T and reacted with HRP-conjugated goat anti-mouse IgG (invitrogen) as a secondary antibody for 1 h at RT. Mouse IgG anti-FLAG M2 (Sigma) and mouse IgG anti-mouse β-actin (Sigma) were used as primary antibodies.

2.11. Immunofluorescence assay

Tail fibroblasts (10^5 cells/well) transduced with the retroviral vectors described above seeded on glass coverslips in a 24-well plate for 20 h at 37 °C. Cells were fixed in 3.7 % paraformaldehyde and permeabilized with 0.2 % Triton X-100 for 10 min each at RT. The cells were blocked with 8 % FBS in PBS for 1 h at RT, followed by incubation with rabbit anti-cRel polyclonal IgG (Santa Cruz) overnight at 4 °C. The cells were washed with PBS and reacted with 1/1000 CF594-conjugated donkey anti-rabbit IgG H&L (Biotium) and DAPI (Nakalai Tesque) for 1 h at RT in the dark. The stained sample was washed six times by PBS and were sealed in Aqueous Mounting Medium, PermaFluor (Fisher Scientific). For tissue staining of germinal center B cells, spleens were fixed in 3.7 % paraformaldehyde for 2 h at 4 °C and then dehydrated in 30 % sucrose/PBS solution (*w*/w) overnight at 4 °C. The sample was embedded in FSC22 Frozen Section Media (Leica) and sectioned at 10 μm using a CM1860 UV (Leica). The sample was blocked in blocking buffer (0.1 % PBST with 0.1 % BSA and 1 % mouse serum) for 1 h at RT and then incubated with Alexa Fluor 488 conjugated lectin PNA (invitrogen), Alexa Flour 594 anti-mouse CD4 (biolegend) and Alexa Flour 647 anti-mouse CD45R/B220 (biolegend) diluted into 1/200 in blocking buffer for 1 h at RT in the dark. The stained sample was washed three times and were sealed in Aqueous Mounting Medium, PermaFluor. The images were observed using FV3000 (Olympus).

2.12. Quantitative RT-PCR

Total RNA was extracted using RNeasy Mini Kit (Qiagen) according to the instructions. RNA was reverse transcribed using Verso cDNA synthesis Kit (Thermo Scientific) according to the instructions. Quantitative PCR was performed on a CFX Connect (Bio-Rad) using GoTaq qPCR Master Mix (Promega) and primers described below. Relative mRNA expression levels were normalized by β-actin and $2^{(-\Delta\Delta Ct)}$ values were calculated.

2.13. Dendritic cells isolation

To increase cell collection, the spleen was injected with 100 U/ml of collagenase D (Roche) in RPMI 1640 and shredded with scissors. Pieces of spleen were digested with 400 U/ml collagenase D solution at 37 °C for 30 min. The digested spleens were mashed in PBS on a 70 μm cell strainer using syringe plunger. After hemolysis with ACK and wash with PBS, dendritic cells were negatively selected using the Pan Dendritic Cell Isolation Kit (Miltenyi Biotec) according to the instructions.

2.14. RNA sequencing

Total RNA was extracted from the negative selected dendritic cells using RNeasy Mini Kit (Qiagen) according to the instructions. Full length cDNA was generated using a SMART-Seq HT Kit (Takara Bio) according to the manufacturer's instructions. An Illumina library was prepared using a Nextera DNA Library Preparation Kit (Illumina) according to the SMARTer kit instructions. Sequencing was performed on an Illumina NovaSeq 6000 sequencer (Illumina) in 101-base single-end mode. Sequenced reads were mapped to the mouse reference genome sequences (mm10) using TopHat v2.0.13 in combination with Bowtie2 ver. 2.2.3 and SAMtools ver. 0.1.19. The fragments per kilobase of exon per million mapped fragments (FPKMs) was calculated using Cufflinks version 2.2.1. Raw count data were analyzed using iDEP.96 with $|\text{FPKM fold change}| > 2.0$ in were considered as differentially expressed genes (DEGs).

2.15. Quantification and statistical analysis

We compared two groups by unpaired two-tailed Student's *t*-test and multiple experimental groups by one-way ANOVA with Turkey multiple comparisons using GraphPad Prism 10.0. Statical significance value are shown as N.S. = not significant, $^*p < 0.05$, $^{**}p < 0.01$ and $^{***}p < 0.001$.

3. Results

3.1. Wild type T. gondii has reduced antibody production with fewer plasma cells compared to Δgra15 T. gondii

C57BL/6 mice were intraperitoneally infected with wild-type *T. gondii* type II (WT *T. gondii*) and GRA15-deficient strain (Δgra15 *T. gondii*) [17]. We first measured specific *T. gondii* antibody titers in sera by ELISA (Fig. 1A). Then both *T. gondii* antibody IgM and IgG levels were

lower in mice infected with WT parasites than those infected with Δgra15 *T. gondii* at 10 days post infection. The number of B cells and plasma cells in the spleen on day 10 of WT or Δgra15 *T. gondii* -infected mice was measured by flow cytometry. Next, the number of $B220^{+}$ $CD138^{-}$ B cells in the spleen showed no significant difference between the WT and Δgra15 *T. gondii* groups (Fig. 1B and C). However, $CD138^{+}$ $B220^{-}$ plasma cells were significantly lower in mice infected with WT parasites than in those infected with Δgra15 *T. gondii*. The GRA15-dependent reduction of plasma cells was consistent with the antibody titer to *T. gondii*.

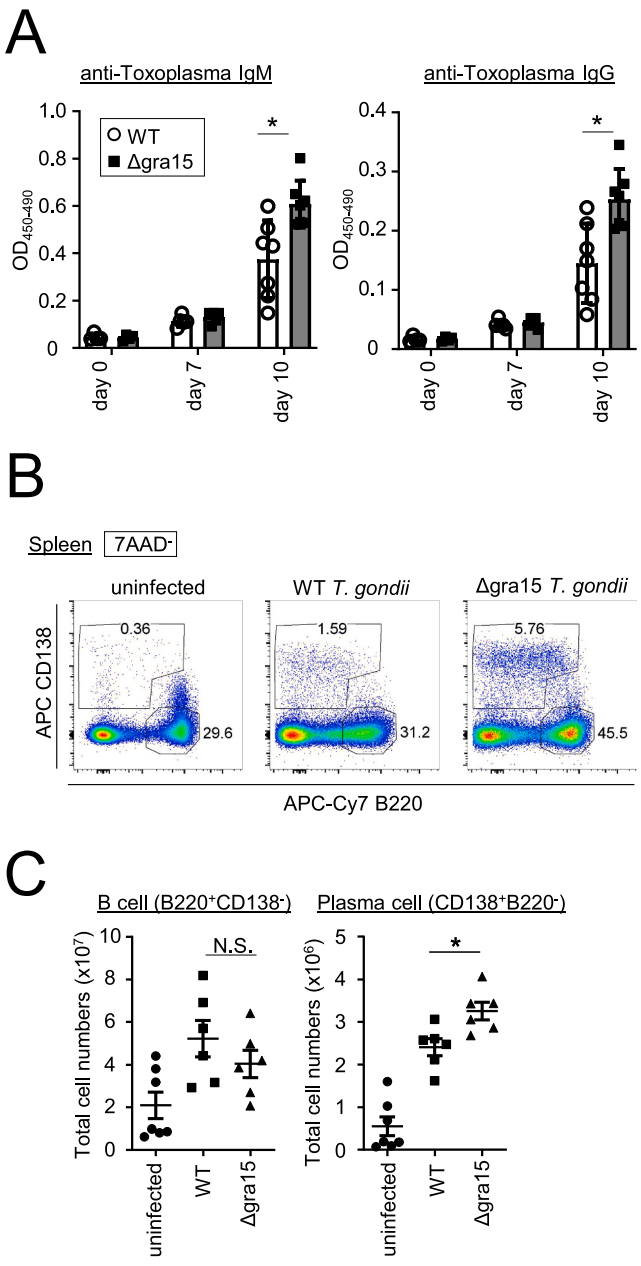

Fig. 1. GRA15 inhibits the production of *T. gondii* antibodies.
(A) Measurement of serum *T. gondii* antibody titers. Anti-*Toxoplasma* IgM and IgG from C57BL/6 mice infected intraperitoneally with wild type (white circles) or Δgra15 *T. gondii* (black squares) on indicated days after infection were measured by ELISA.
(B and C) Flow cytometric analysis of spleen 10 days after intraperitoneal infection of C57BL/6 mice with wild type or Δgra15 *T. gondii* with their plot diagram (B) and B cell count (C). The black line in the plot diagram refers to B cells ($B220^{+}CD138^{-}$) and plasma cell ($CD138^{+}B220^{-}$), and the numbers indicate the percentage of them among live cells.
Error bars represent SD. $^{*}p < 0.05$, N.S.: not significant.

3.2. Generation of conditional knock-in mice with forced expression of GRA15 in specific cells

We tried to examine the mechanism of the antibody suppression to *T. gondii*, however, it is difficult to distinguish *in vivo* the immune cell types that suppress B cells by GRA15 in wild-type parasites, because *T. gondii* can infect all nucleated cells. Therefore, we generated conditional knock-in mice in which GRA15 is expressed only in specific cells by applying the Cre-loxP system (Fig. 2A). The mice had loxP-STOP-loxP (LSL), GRA15 and FLAG sequences inserted into the ROSA26 locus by CRISPR-Cas9 genome editing. From now on, these knock-in mice will be called LSL-GRA15 mice. In these mice, GRA15-FLAG was supposed to expressed only in Cre-expressing cells. To assess GRA15 expression, Cre were introduced into the tail fibroblasts of C57BL/6 mice and LSL-GRA15 mice using retrovirus vector. Expression of GRA15-FLAG was assessed by western blotting (Fig. 2B). Expression of GRA15-FLAG was only detected when Cre was expressed in LSL-GRA15 mice derived cells. Next, functionality of the expressed GRA15 was determined by immunofluorescence assay for NF-κB activation (Fig. 2C). GRA15 was shown to activate the cRel NF-κB subunit and induce its translocation into nucleus [16]. Immunofluorescence assay exhibited that cRel translocation into the nucleus in the Cre-transfected LSL-GRA15 tail fibroblasts, but not in control empty vector-transfected cells (Fig. 2C). These data suggest conditional expression of the functional GRA15 in LSL-GRA15 mice.

3.3. GRA15 expression on macrophages does not cause GRA15-dependent decrease in antibody titer

T. gondii mainly infects macrophages *in vivo*. To investigate the role of GRA15 in macrophages, the LSL-GRA15 mice were crossed with LysM-Cre mice, resulting in the generation of LysM-Cre/LSL-GRA15 mice (Fig. 2A). We first performed reverse transcription quantitative PCR (RT-qPCR) to test whether GRA15 was expressed in bone marrow-derived macrophages (BMDM) from LysM-Cre/LSL-GRA15 mice (Fig. 2D). We found GRA15 mRNA expression in BMDM from LysM-Cre/LSL-GRA15 mice but not in those from control mice. When anti-*T. gondii* IgM and IgG titers were assessed after Δgra15 *T. gondii* infection, there were no significant changes between LysM-Cre/LSL-GRA15 mice and the control mice (Fig. 2E). Moreover, there were no significant differences in the total cell number of B cells and plasma cells under infected conditions (Fig. S2A and B). These results suggested that GRA15 expression in macrophages does not account for the suppression of B cell-dependent immune response.

3.4. GRA15 expression on dendritic cells causes GRA15-dependent decrease in antibody titer

Not only macrophages but also DCs are important innate immune cells targeted by *T. gondii in vivo* [30–32]. To investigate the consequence of GRA15 in DCs, the LSL-GRA15 mice were crossed with CD11c-Cre mice, resulting in the generation of CD11c-Cre/LSL-GRA15 mice (Fig. 2A). We performed RT-qPCR of GRA15 in splenic DCs from CD11c-Cre/LSL-GRA15 mice (Fig. 3A). We found GRA15 mRNA in splenic DCs from CD11c-Cre/LSL-GRA15 mice but not in those from control mice. Next, anti-*T. gondii* IgM and IgG were measured after Δgra15 *T. gondii* infection (Fig. 3B). It was noteworthy that anti-*T. gondii* IgM and IgG antibody titers were lower in the infected CD11c-Cre/LSL-GRA15 mice than in control mice. The number of plasma cells measured by flow cytometry was also reduced in the infected CD11c-Cre/LSL-GRA15 mice compared to the infected control mice (Fig. 3C and D). There were no significant differences in the number of B cells or plasma cells in the uninfected state between control and CD11c-Cre/LSL-GRA15 mice. This

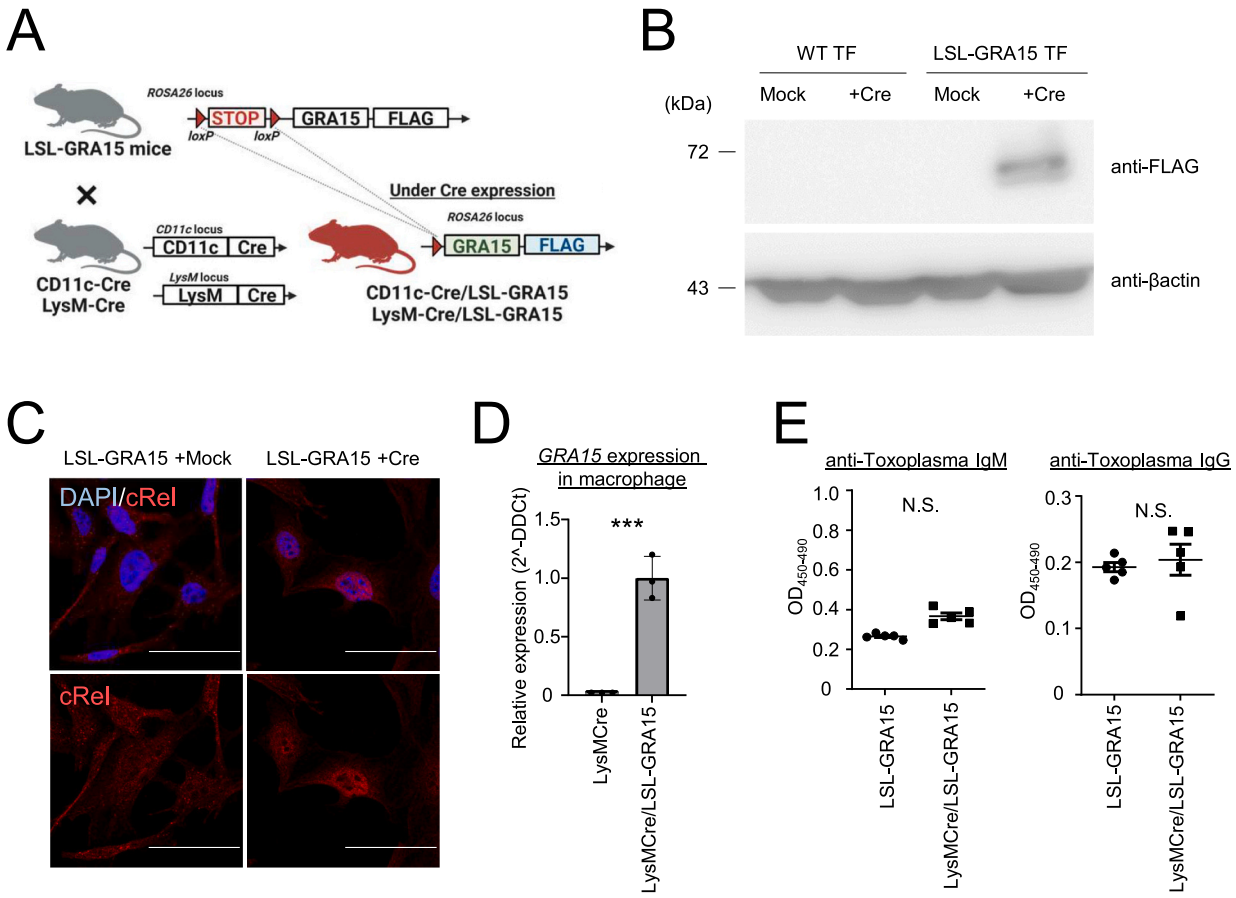

Fig. 2. Generation of Rosa26 LSL-GRA15 conditional knock in mice.
(A) Schematic of the principle of gene expression in LSL-GRA15 conditional knock in mice (LSL-GRA15). By crossing LysM-Cre or CD11c-Cre mice, LSL-GRA15 mice express GRA15 only in Cre-expressing macrophages or dendritic cells.
(B and C) Western blot and immunofluorescence microscopy of functional FLAG tagged GRA15 expression in LSL-GRA15 mice. Cre were introduced into the tail fibroblasts (TF) of C57BL/6 mice and LSL-GRA15 mice using retrovirus vector. (B) Western blotting was used to analyze the expression of FLAG and β-actin in TF cells transfected with Cre or Mock. (C) Immunofluorescence microscopy was used to determine whether nuclear translocation of NF-κB could be induced by GRA15 in LSL-GRA15 mice. The TF cells stained with anti-cRel (red) and DAPI (blue). Scale bar is 50 μm.
(D) RT-qPCR analysis of *gra15* gene expression with *β-actin* as the endogenous control in bone marrow derived macrophages from LysM-Cre and LysM-Cre/LSL-GRA15 mice. Expression level was calculated using the comparative cycle threshold ($2^{-\Delta\Delta Ct}$) value method.
(E) Measurement of serum *T. gondii* antibody titers. Anti-*Toxoplasma* IgM and IgG from control or LysM-Cre/LSL-GRA15 mice infected intraperitoneally with Δgra15 *T. gondii* on 9 days after infection were measured by ELISA.
Error bars represent SD. ***$p < 0.001$, N.S.: not significant. (For interpretation of the references to colour in this figure legend, the reader is referred to the web version of this article.)

is reminiscent of the data obtained when C57BL/6 mice were infected with WT parasites (Fig. 1A-C). These results suggest that GRA15-dependent suppression of B cell responses might be mediated by GRA15 expression in DCs but not in macrophages.

3.5. *GRA15 in dendritic cells suppresses antibody production even with T cell-dependent antigens*

Next, to assess whether the GRA15-dependent suppression of B cell responses requires parasite infection. We used OVA protein administrated intravenously into control and CD11c-Cre/LSL-GRA15 mice. Serum anti-OVA IgM/IgG antibody titers were evaluated by ELISA (Fig. 4A). Both IgM and IgG OVA antibody titers in CD11c-Cre/LSL-GRA15 mice were lower than in control mice at 8 and 15 days. Next, the splenic B cells at 15 days after treatment were analyzed by flow cytometry (Fig. 4B and C). The numbers of germinal center (GC) B cells were severely reduced in CD11c-Cre/LSL-GRA15 mice than in control, whereas there was no significant difference in the number of B cells and plasma cells. It is known that both plasma cells and GC B cells are directly involved in the production of specific antibodies [33]. Thus, the suppression of specific antibody titers by GRA15 was not related to infection. Since OVA protein is a T cell-dependent antigen, we next evaluated H-2K^b OVA tetramer on CD8$^+$ T cells in the spleen of control and CD11c-Cre/LSL-GRA15 mice 5 days after OVA administration by flow cytometry (Fig. 4D). H-2K^b OVA tetramer$^+$ CD8$^+$ T cells were reduced in OVA-treated CD11c-Cre/LSL-GRA15 mice compared to OVA-treated control mice. OVA tetramer$^+$CD4$^+$ T cells could not be detected in either OVA-treated control mice or CD11c-Cre/LSL-GRA15 mice due to the sensitivity limitations of the antibodies (data not shown). Subsequently, the germinal center B cells and CD4$^+$ T cells in the spleens of control and CD11c-Cre/LSL-GRA15 mice on day 14 after OVA administration were observed using immunohistochemistry (Fig. 4E and F). In the OVA-treated control mice, PNA$^+$B220$^+$ germinal center B cells were adequately formed and showed a significant presence of CD4$^+$ T cells inside. In contrast, the CD11c-Cre/LSL-GRA15 mice had insufficient germinal center B cell formation. However, there were no significant differences in the number of Bcl-6$^+$ follicular helper T or GATA3$^+$ Th2 in the spleen between the control and the CD11c-Cre/LSL-GRA15 mice after OVA immunization (sFig. 3). In addition, there were significant differences in the *in vitro* proliferation rate or cytokine production of T

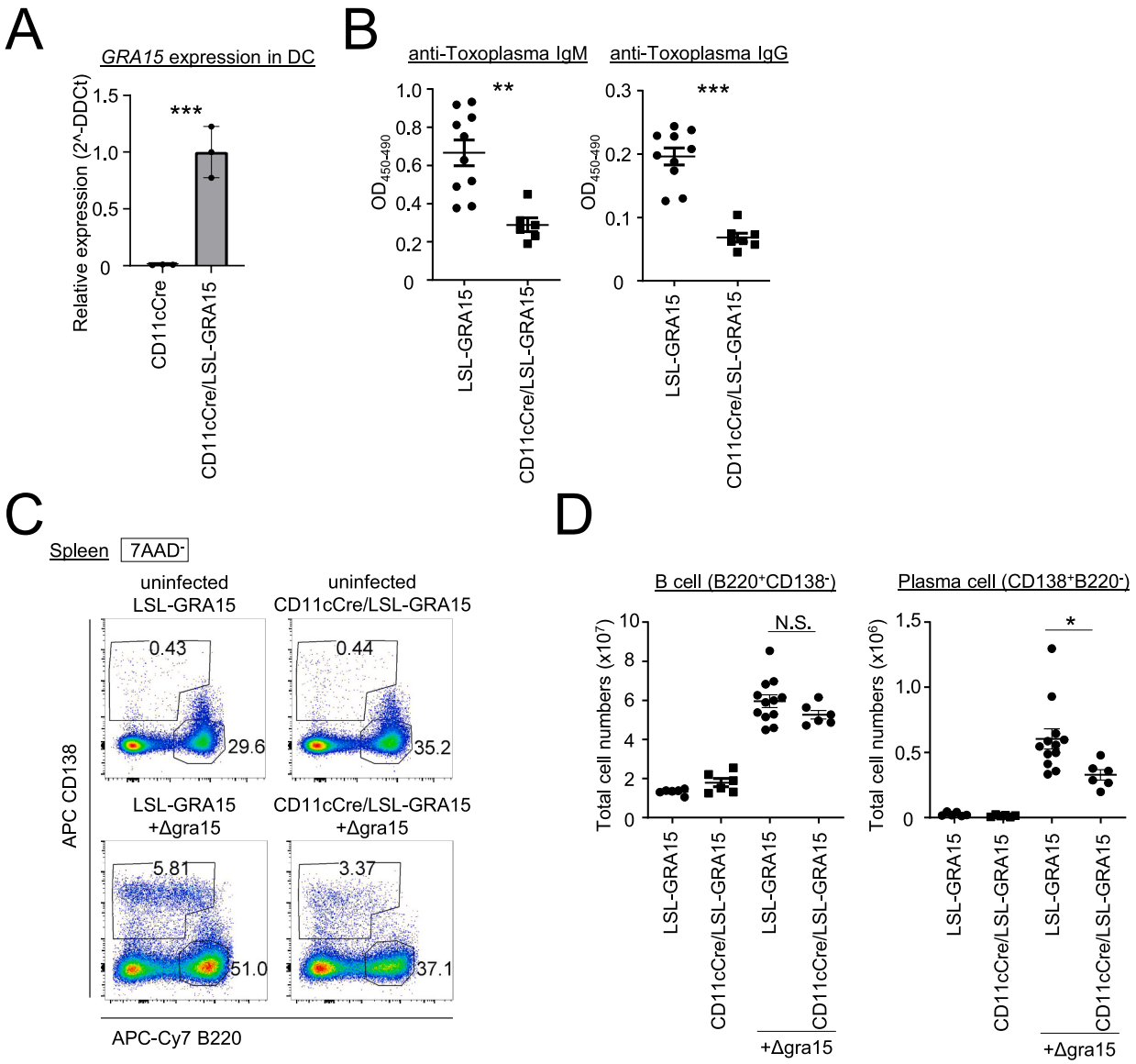

Fig. 3. GRA15 expression in dendritic cells suppresses the production of *T. gondii* antibodies.
(A) RT-qPCR analysis of *gra15* gene expression with *β-actin* as the endogenous control in the splenic dendritic cell from CD11c-Cre and CD11c-Cre/LSL-GRA15 mice. Expression level was calculated using the comparative cycle threshold ($2^{-\Delta\Delta Ct}$) value method.
(B) Measurement of serum *T. gondii* antibody titers. Anti-*Toxoplasma* IgM and IgG from control or CD11c-Cre/LSL-GRA15 mice infected intraperitoneally with Δgra15 *T. gondii* on 9 days after infection were measured by ELISA.
(C and D) Flow cytometric analysis of spleen 9 days after intraperitoneal infection of CD11c-Cre and CD11c-Cre/LSL-GRA15 mice with Δgra15 *T. gondii* with their plot diagram (C) and B cell count (D). The black line in the plot diagram refers to B cells and plasma cell, and the numbers indicate the percentage of them among live cells.
Error bars represent SD. *p < 0.05, **p < 0.01, ***p < 0.001, N.S.: not significant.

cells co-cultured with the respective dendritic cells (data not shown).

Next, we investigated whether GRA15 also induces a reduction in antibody production against T cell-independent NP-Ficoll antigen (Fig. 5A). In contrast to the data using OVA protein, there was no significant difference in antibody titers between control and CD11c-Cre/LSL-GRA15 mice at day 14 after NP-Ficoll administration. The numbers of B cell, plasma cell and GC B cell were also not statistically different between the two groups (Fig. 5B and C). Taken together, these results indicate that GRA15 expression in DCs mediates suppression of adaptive immune responses to T cell dependent antigen independently of infection.

3.6. GRA15 increases inhibitory receptor expression on the surface of T cells

We attempted to elucidate the mechanism by which GRA15 expressed in DCs suppresses the adaptive immune responses. First, we investigated inhibitory receptors on T cells, such as programmed cell death protein 1 (PD-1), T cell immunoreceptor with Ig and ITIM domains (TIGIT) and Lymphocyte Activation Gene-3 (LAG-3), from control or CD11c-Cre/LSL-GRA15 mice by flow cytometry (Fig. 6A and B). The PD-1, TIGIT and LAG-3 positive proportion of $CD4^+$ T cells and $CD8^+$ T cells were higher in CD11c-Cre/LSL-GRA15 mice than in control mice. The expression levels of PD-1, TIGIT, and LAG3 in T cells during WT or Δgra15 *T. gondii* infection were also examined. The number of PD-1^+ T cells in the peritoneal exudate cells of WT parasites infection was higher

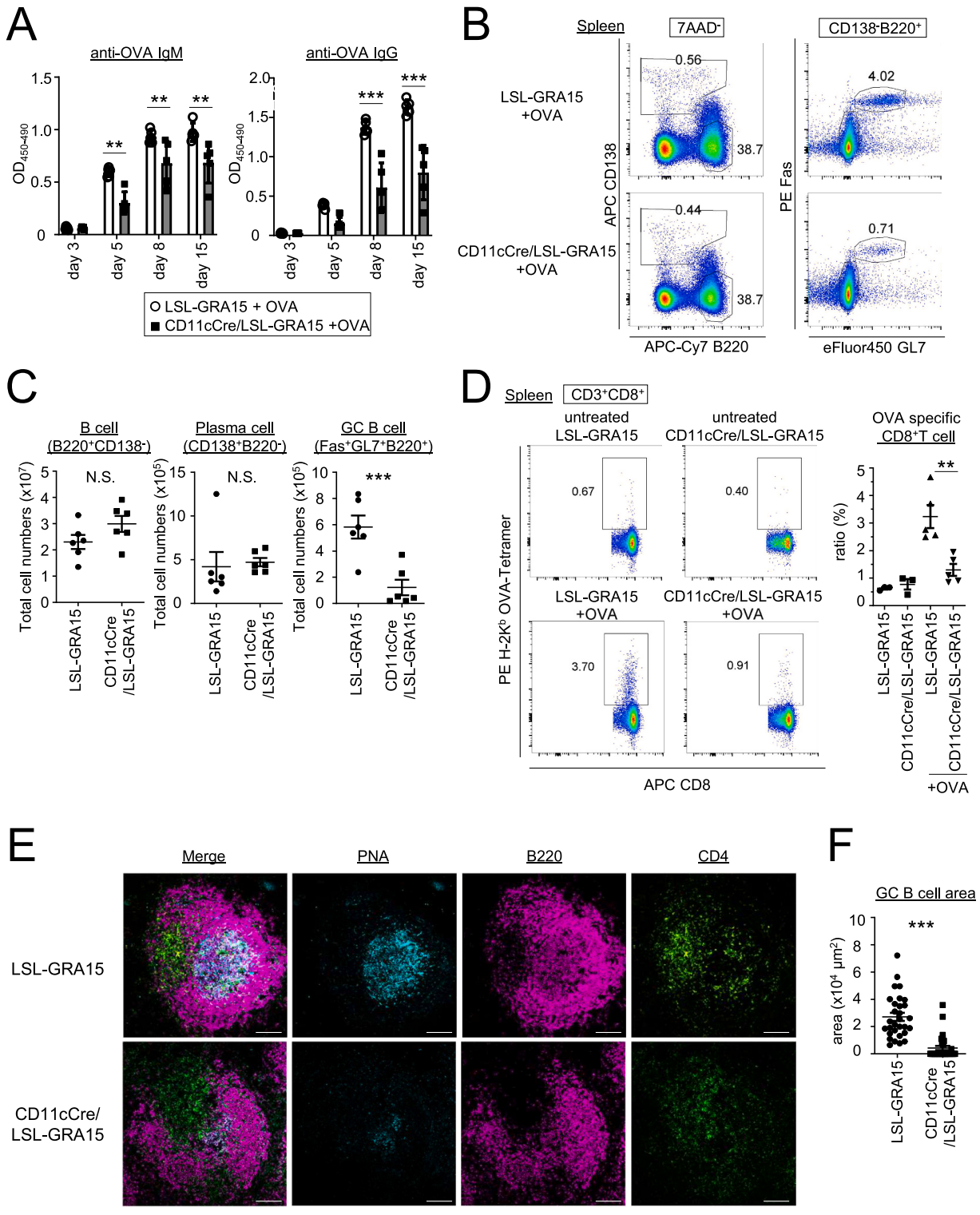

Fig. 4. GRA15 expression in dendritic cells suppresses the production of anti-OVA antibodies.
(A) Measurement of serum OVA antibody titers. Anti-OVA IgM and IgG from control or CD11c-Cre/LSL-GRA15 mice treated with OVA protein and poly (I:C) on indicated days were measured by ELISA.
(B and C) Flow cytometric analysis of spleen 15 days after treatment of control and CD11c-Cre/LSL-GRA15 mice with OVA protein and poly (I:C) with their plot diagram (B) and B cell count (C). The black line and number in the plot diagram refer to the ratio of B cells, plasma cell and germinal center (GC) B cell ($Fas^+GL7^+B220^+$).
(D) Flow cytometric analysis of spleen 5 days after treatment of control and CD11c-Cre/LSL-GRA15 mice with OVA protein and poly (I:C) with their plot diagram and OVA-Tetramer$^+$ $CD8^+$ T cell ratio. The black line and number in the plot diagram refer to OVA-Tetramer$^+$ $CD8^+$ T cell among $CD8^+$ T cells.
(E and F) Immunofluorescence microscopy of the spleen of 14 days after treatment of control and CD11c-Cre/LSL-GRA15 mice with OVA protein and poly (I:C). The spleen stained with anti-PNA (cyan), anti-B220 (magenta) and anti-CD4 (green). The white square area is magnified in the upper left corner. Scale bar is 100 μm. Error bars represent SD. $^{**}p < 0.01$, $^{***}p < 0.001$, N.S.: not significant. (For interpretation of the references to colour in this figure legend, the reader is referred to the web version of this article.)

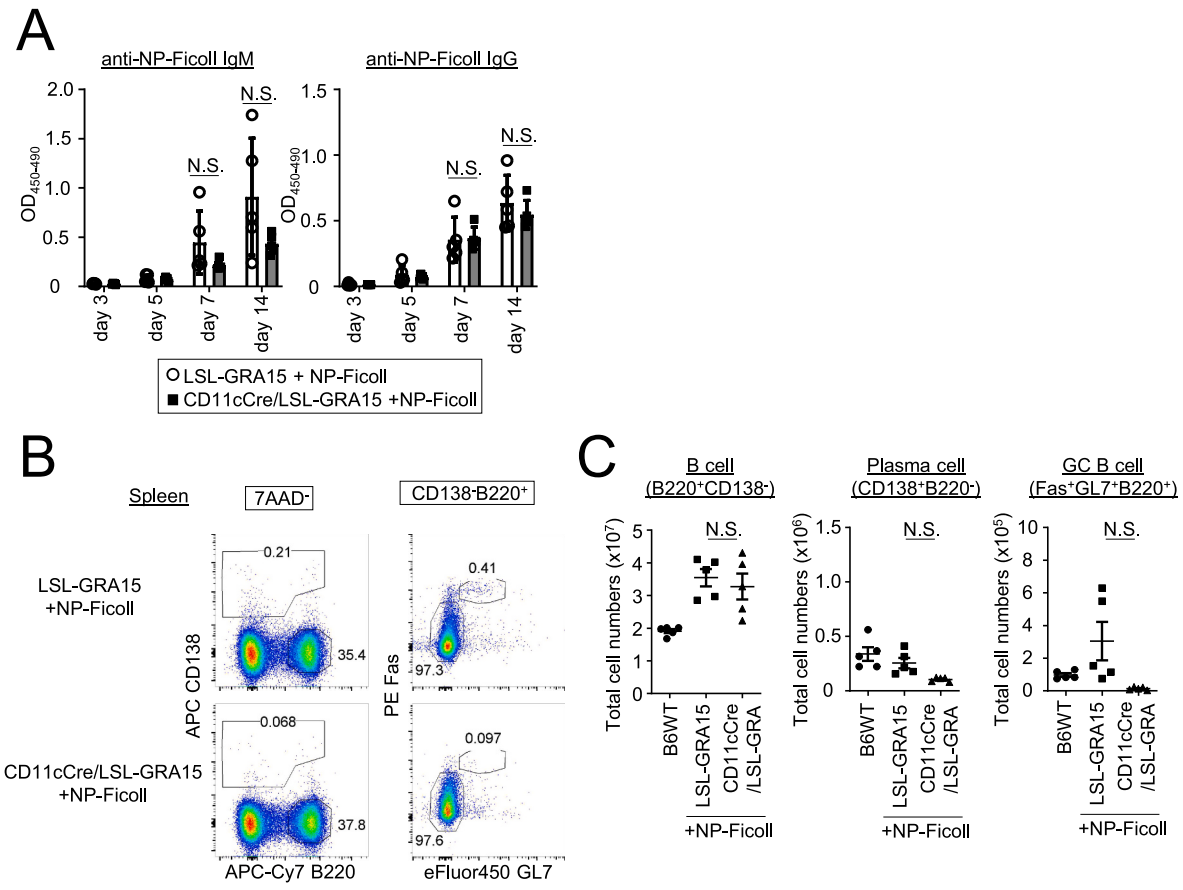

Fig. 5. GRA15 expression in dendritic cells does not suppresses the production of anti-NP-Ficoll antibodies.
(A) Measurement of serum NP-Ficoll antibody titers. Anti- NP-Ficoll IgM and IgG from control or CD11c-Cre/LSL-GRA15 mice treated with NP-Ficoll protein and poly (I:C) on indicated days were measured by ELISA.
(B and C) Flow cytometric analysis of spleen 14 days after treatment of control and CD11c-Cre/LSL-GRA15 mice with NP-Ficoll protein and poly (I:C) with their plot diagram (B) and B cell count (C). The black line and number in the plot diagram refer to the ratio of B cells, plasma cell and germinal center (GC) B cell ($Fas^+GL7^+B220^+$).

than that of Δgra15 *T. gondii* on day 5 after infection (Fig. 6C and D), although there was no significant difference in the number of PD-1^+ T cells in the spleen between WT parasites and Δgra15 *T. gondii* (data not shown). In addition, PD-1^+ T cells of PEC in WT parasites infection did not express TIGIT, LAG-3 and CTLA4 (data not shown).

Additionally, we conducted bulk RNA sequencing of DCs in the spleens of control and CD11c-Cre/LSL-GRA15 mice (Fig. 7A and B). The expression of numerous target genes of the NF-κB pathway, including chemokines, cytokines, complement, and IFN-induced guanylate-binding proteins (GBPs), was elevated in CD11c-Cre/LSL-GRA15 mice (Fig. 7B). The findings indicated that the expression of GRA15 can induce host immune activation in DCs without infection.

4. Discussion

The main function of GRA15 was thought to be activation of the host's innate immune system. GRA15 has been demonstrated to induce the secretion of inflammatory cytokines from infected macrophages [15–17]. Additionally, GRA15 has been shown to enhance ICAM-1 expression in infected DCs [34], and ICAM-1 promotes immune synapses formation in DCs and T cells [35,36]. In oral infection, GRA15 also strongly induces intestinal inflammation [37]. GRA15 exhibits host-friendly characteristics; however, the distribution of type II *T. gondii* is more extensive than that of type I (RH strain), which does not express GRA15. Many previous papers claim roles for GRA15 in modulating immunity and spreading infection without killing the host. However, this claim has not been specifically proven. In this article, we showed that expression of GRA15 in DCs suppressed the production of specific *T. gondii* antibodies. Suppression of antibody production is a clear benefit of GRA15. This suppression of antibody production by GRA15 was also observed in CD11c-Cre/LSL-GRA15 mice immunized with OVA. This indicates that it is a direct consequence of GRA15, rather than an indirect effect resulting from the infection of Δgra15 *T. gondii*. There is a report that the number of cysts in the brain drops dramatically when *T. gondii* antibodies are high following vaccination against cyst wall proteins [38]. GRA15 might play a role in the promotion of cyst formation within tissues by virtue of its ability to inhibit antibody production. However, the number of cysts was not evaluated in this study, as the parasites utilized in our experiment could not form cysts. In this study, PD-1^+ $TIGIT^+$ LAG-3^+ T cells were increased in CD11c-Cre/LSL-GRA15 mice. Merritt et al. also reported an increase in $PD1^+CTLA4^+$ T cells in a GRA15-dependent manner [39], and it is possible that the excessive activation of immunity by GRA15 induces T cell exhaustion. However, in our study, T cells expressing immunosuppressive receptors other than PD-1 did not increase during infection with WT parasites. Since PD-1 is also expressed on activated T cells [40], no definitive conclusion can be drawn regarding the impact of GRA15 on T cell exhaustion.

We employed a methodology based on the expression of GRA15 in host cells, with the objective of evaluating its impact on the immune system *in vivo*. While there are studies using mice ectopically expressing virulence factors such as the CagA protein of *Helicobacter pylori* and the E6 protein of human papillomavirus [41,42], a similar approach has not been used in the studies of *T. gondii* parasitology. In a previous study,

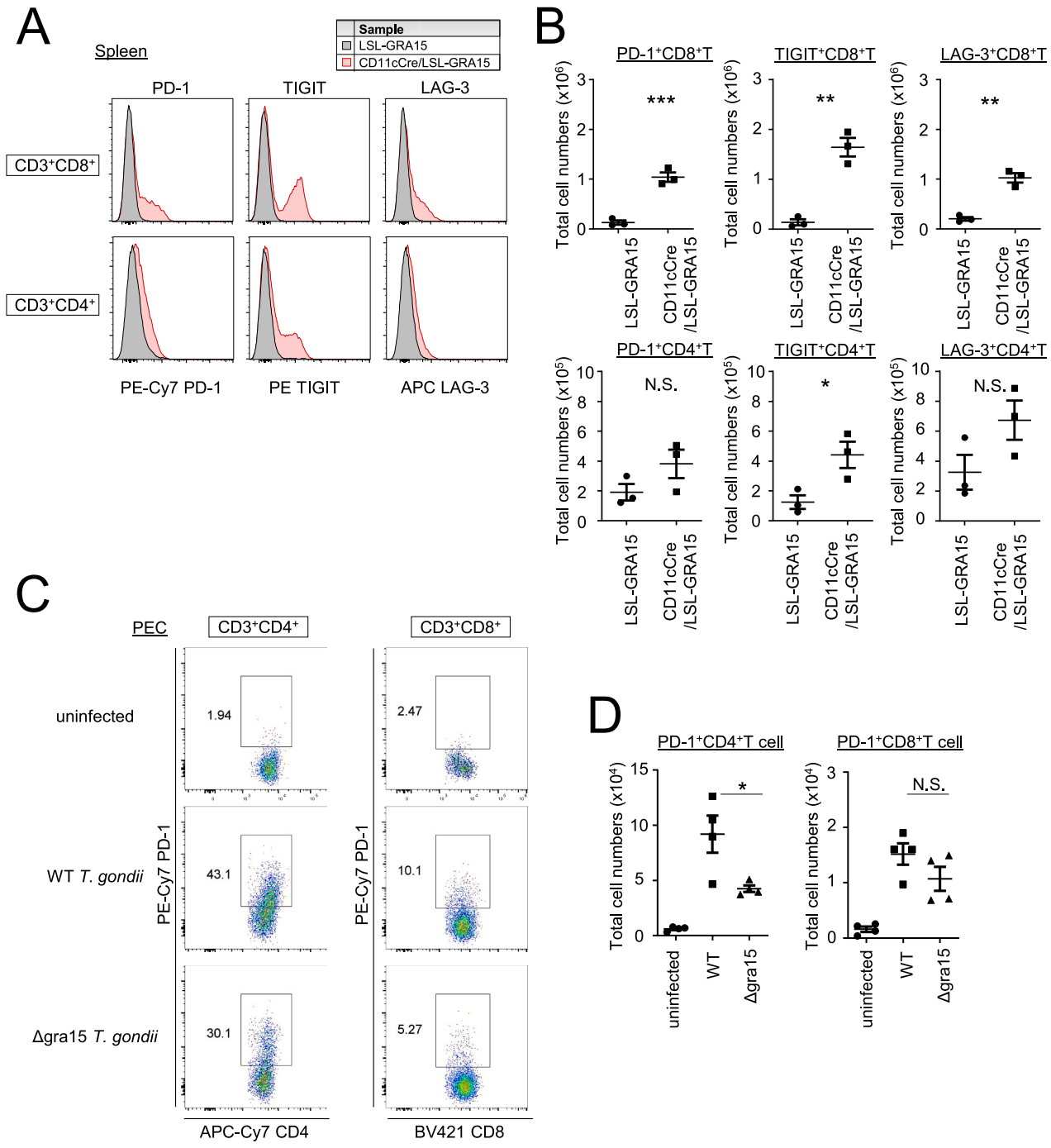

Fig. 6. GRA15 induces expression of inhibitory receptors on T cells.
(A and B) Flow cytometric analysis of spleen in control (black) and CD11c-Cre/LSL-GRA15 mice (red) with their plot diagram (A) and the number of $CD8^+$ T and $CD4^+$ T cells expressing PD-1, TIGIT and LAG-3 (B).
(C and D) Flow cytometric analysis of peritoneal exudate cells 5 days after intraperitoneal infection of C57BL/6 mice with wild type or Δgra15 *T. gondii* with their plot diagram (C) and PD-1^+ $CD8^+$ T and PD-1^+ $CD4^+$ T cell count (D).
Error bars represent SD. *$p < 0.05$, **$p < 0.01$, ***$p < 0.001$, N.S.: not significant. (For interpretation of the references to colour in this figure legend, the reader is referred to the web version of this article.)

bulk RNA-seq of hamster kidney BHK-21 cell line and immortalized BMDM overexpressing type II GRA15 were conducted to demonstrate the impact of NF-κB activation *in vitro* [43,44]. Therefore, the value of our study lies in its evaluation of GRA15 function in mouse DCs but not cell line. The results of our RNA-seq analysis indicated that four genes (*Igfbp5, Medag, Pdpn, and Sphk1*) and IFNβ-inducible genes (*Irf1, Gbp2 and Gbp3*) were upregulated as previously observed in BHK-21 cells and immortalized BMDM, respectively. Additionally, the expression of inflammatory genes such as chemokines/cytokines (*Ccl8, Ccl12, Cxcl9, Cxcl10*, *Il1a* and *Il33*) and the complement system (*C1ra, C1s1, C2, C3, C4b, Cfb and Serping1*) were markedly elevated. It is noteworthy that a significant increase was observed in IFNβ-inducible genes (*Gbp2, Gbp2b, Gbp3, Gbp5, Gbp6, Gbp,7 Gbp10, Ifi44, Ifi47, Igtp, Irf1, Irgm1, Oas2, Oasl2, Nos2, Tgtp1* and *Tgtp2*). While the bulk RNA-seq data indicated that immune suppressive genes such as *Cd274 (Pdl1)*, *Pdcd1lg2 (Pdl2)*, *Tgfb1* and *Il10* were not involved in the GRA15-induced inhibition of the

A

Enriched pathways in DEGs for the selected comparison:

Direction	adj.Pval	nGenes	Pathways
Down regulated	4.5e-03	7	Positive regulation of cation transmembrane transport
	4.5e-03	8	Regulation of calcium ion transport
	8.9e-03	9	Calcium ion transport
	8.9e-03	9	Regulation of metal ion transport
Up regulated	1.3e-18	42	Defense response
	2.8e-17	13	Cellular response to interferon-beta
	6.0e-17	38	Response to external biotic stimulus
	6.0e-17	38	Response to other organism
	9.5e-17	40	Immune response
	1.6e-16	13	Response to interferon-beta
	3.6e-16	31	Response to cytokine
	4.4e-16	38	Biological process involved in interspecies interaction between organisms
	1.5e-15	47	Immune system process
	3.3e-15	31	Defense response to other organism
	3.3e-15	48	Response to external stimulus
	8.0e-15	27	Response to bacterium
	3.7e-14	44	Cellular response to organic substance
	5.6e-14	27	Cellular response to cytokine stimulus
	7.6e-14	53	Response to stress

B

Function	Upregulated gene in CD11c-Cre/LSL-GRA15 mice									
Cytokine/Chemokine	*Ccl12*	*Ccl19*	*Ccl8*	*Cxcl10*	*Cxcl11*	*Cxcl9*	*Il1a*	*Il33*		
Complement System	*C1ra*	*C1s1*	*C2*	*C3*	*C4b*	*Cfb*	*Serping1*			
IFN inducible genes	*Gbp2*	*Gbp2b*	*Gbp3*	*Gbp5*	*Gbp6*	*Gbp7*	*Gbp10*	*Ifi44*	*Ifi47*	*Igtp*	*Iigp1*
	Irf1	*Irgm1*	*Nos2*	*Oas2*	*Oasl2*	*Tgtp1*	*Tgtp2*			
Apotosis promotor	*Batf2*	*Casp12*	*Cst7*	*Fhl1*	*Gadd45b*					
Apotosis inhibitor	*Naip1*									
Enzyme/Metabolism	*Aoah*	*Aqp1*	*Car2*	*Cox6a2*	*Epx*	*Gpx8*	*Htra1*	*Lyz1*	*Pcsk6*	*Pla2g2d*	*Sphk1*
Cell surface marker/receptor	*Cdh11*	*Colec12*	*Igfbp2*	*Igfbp5*	*Mpzl2*	*Pdpn*	*Pmp22*	*Tspan7*	*Upk3b*		
Others	*Hspa12a*	*Medag*	*Saa3*	*Snhg9*						

Function	Downregulated gene in CD11c-Cre/LSL-GRA15 mice					
Enzyme/Metabolism	*Nos1*					
Cell surface marker/receptor	*Cacna1d*	*Cacna1h*	*Cd19*	*Fcrl5*	*Kcnc1*	*Oprd1*
Others	*Arc*	*Ehd3*	*Gramd2*	*Stac2*		

Fig. 7. RNA sequencing of dendritic cells from CD11cCre/LSL-GRA15 mice.
(A and B) Dendritic cells from the spleens of control and CD11c-Cre/LSL-GRA15 mice were collected by negative magnetic selection, and gene expression was compared by bulk-RNA sequencing. Gene Ontology analysis of up- or down-regulated genes in dendritic cells of CD11cCre/LSL-GRA15 mice (A) and table of major genes (B).

adaptive immune responses, the data might contain genes involved in unidentified suppressive mechanisms. However, there are several limitations to this study. We have shown that GRA15 in dendritic cells somehow suppresses acquired immunity, but we have not been able to determine how it suppresses T cells and B cells. Furthermore, The CD11c-Cre/LSL-GRA15 mice model exhibits high GRA15 expression in $CD11c^{+}$ cells since the time of birth. This would be expected to exceed the amount and duration of GRA15 expression during *Toxoplasma* infection and might not reproduce GRA15 function during infection.

The only vaccine in practical use is Toxovax, an attenuated live attenuated vaccine for sheep using S48 strain [45]. However, it is unclear when the S48 strain might regain virulence. As an alternative, a gene-deficient type II *Toxoplasma* strain containing alpha-amylase and adenyl succinate lyase has been proposed as a potential replacement for the S48 strain [46,47]. Although not examined in this study, the presence of GRA15 may act to suppress secondary antibody production during a second infection. This may be an obstacle to the development of a live *Toxoplasma* vaccine. Developing a live attenuated *Toxoplasma* type II vaccine with double knockout of both α-amylase or adenylosuccinate lyase, as well as GRA15, could potentially result in a vaccine with enhanced the ability to significantly boost *Toxoplasma*-specific antibodies.

We found that when GRA15 is expressed on DCs, specific antibody production is significantly reduced. In addition, GRA15 suppressed T cell-dependent humoral immune responses, a mechanism that was also suggested to be influenced by increased expression of immunosuppressive receptors. This study shows novel pathological significance of GRA15 and might have potential application in the development of *T. gondii* vaccines.

CRediT authorship contribution statement

Yuki Nakayama: Writing – review & editing, Writing – original draft, Visualization, Validation, Investigation, Formal analysis, Data curation, Conceptualization. **Fumiaki Ihara:** Methodology. **Daisuke Okuzaki:** Methodology, Data curation. **Yoshifumi Nishikawa:** Resources. **Miwa Sasai:** Methodology, Funding acquisition, Formal analysis, Conceptualization. **Masahiro Yamamoto:** Writing – review & editing, Writing – original draft, Supervision, Project administration, Funding acquisition, Formal analysis, Conceptualization.

Declaration of competing interest

The authors have no conflicting financial interests to declare.

Acknowledgments

We thank Mari Enomoto and Nodoka Yamagishi (Osaka University) for secretarial assistance. We thank Prof. Tomohiro Kurosaki and Associate Prof. Takeshi Inoue (Laboratory of Lymphocyte Differentiation, Osaka University) for some advice on B cells. This study was supported by Japan Science and Technology Agency (JPMJFR206D and JPMJMS2025); Agency for Medical Research and Development (JP24fk0108682, and JP223fa627002); Ministry of Education, Culture, Sports, Science and Technology (20B304 and 19H00970); the program from Joint Usage and Joint Research Programs of the Institute of Advanced Medical Sciences, Tokushima University; Takeda Science Foundation; Mochida Memorial Foundation; Astellas Foundation for Research on Metabolic Disorders; Naito Foundation; the Chemo-Sero-Therapeutic Research Institute; Research Foundation for Microbial Diseases of Osaka University; BIKEN Taniguchi Scholarship; The Nippon Foundation - Osaka University Project for Infectious Disease Prevention; and Joint Research Program of Research Center for Global and Local Infectious Diseases of Oita University (2021B06).

Appendix A. Supplementary data

Supplementary data to this article can be found online at https://doi.org/10.1016/j.parint.2024.102995.

References

[1] G. Milne, J.P. Webster, M. Walker, Toxoplasma gondii: an underestimated threat? Trends Parasitol. 36 (2020) 959–969, https://doi.org/10.1016/j.pt.2020.08.005.
[2] M. Attias, D.E. Teixeira, M. Benchimol, R.C. Vommaro, P.H. Crepaldi, W. De Souza, The life-cycle of toxoplasma gondii reviewed using animations, Parasit. Vectors 13 (2020) 588, https://doi.org/10.1186/s13071-020-04445-z.
[3] Y. Zhang, B.S. Lai, M. Juhas, Y. Zhang, Toxoplasma gondii secretory proteins and their role in invasion and pathogenesis, Microbiol. Res. 10 (2019) 126923, https://doi.org/10.1016/j.micres.2019.06.003.
[4] T.S. Lima, M.B. Lodoen, Mechanisms of human innate immune evasion by toxoplasma gondii, Front. Cell. Infect. Microbiol. 9 (2019) 103, https://doi.org/10.3389/fcimb.2019.00103.
[5] I.A. Khan, M. Moretto, Immune responses to toxoplasma gondii, Curr. Opin. Immunol. 77 (2022) 102226, https://doi.org/10.1016/j.coi.2022.102226.
[6] M.S. Behnke, S.J. Fentress, M. Mashayekhi, L.X. Li, G.A. Taylor, L.D. Sibley, The polymorphic pseudokinase ROP5 controls virulence in toxoplasma gondii by regulating the active kinase ROP18, PLoS Pathog. 8 (2012) e1002992, https://doi.org/10.1371/journal.ppat.1002992.
[7] R.D. Etheridge, A. Alaganan, K. Tang, H.J. Lou, B.E. Turk, L.D. Sibley, The toxoplasma pseudokinase ROP5 forms complexes with ROP18 and ROP17 kinases that synergize to control acute virulence in mice, Cell Host Microbe 15 (2014) 537–550, https://doi.org/10.1016/j.chom.2014.04.002.
[8] Y. Lee, H. Yamada, A. Pradipta, J.S. Ma, M. Okamoto, H. Nagaoka, E. Takashima, D.M. Standley, M. Sasai, K. Takei, M. Yamamoto, Initial phospholipid-dependent Irgb6 targeting to toxoplasma gondii vacuoles mediates host defense, Life Sci. Alliance 3 (2020) e201900549, https://doi.org/10.26508/lsa.201900549.
[9] T. Steinfeldt, S. Könen-Waisman, L. Tong, N. Pawlowski, T. Lamkemeyer, L. D. Sibley, J.P. Hunn, J.C. Howard, Phosphorylation of mouse immunity-related gtpase (IRG) resistance proteins is an evasion strategy for virulent toxoplasma gondii, PLoS Biol. 8 (2010) e1000576, https://doi.org/10.1371/journal.pbio.1000576.
[10] J. Sibert, J. Hampton, P. Kleiber, M. Maunder, Biomass, size, and trophic status of top predators in the Pacific Ocean, Science 314 (2006) (1979) 1773–1776, https://doi.org/10.1126/science.1135347.
[11] Y.C. Ong, M.L. Reese, J.C. Boothroyd, Toxoplasma rhoptry protein 16 (ROP16) subverts host function by direct tyrosine phosphorylation of STAT6, J. Biol. Chem. 285 (2010) 28731–28740, https://doi.org/10.1074/jbc.M110.112359.
[12] J.P.J. Saeij, S. Coller, J.P. Boyle, M.E. Jerome, M.W. White, J.C. Boothroyd, Toxoplasma co-opts host gene expression by injection of a polymorphic kinase homologue, Nature 445 (2007) 324–327, https://doi.org/10.1038/nature05395.
[13] P. Olias, R.D. Etheridge, Y. Zhang, M.J. Holtzman, L.D. Sibley, Toxoplasma effector recruits the Mi-2/NuRD complex to repress STAT1 transcription and block IFN-γ-dependent gene expression, Cell Host Microbe 20 (2016) 72–82, https://doi.org/10.1016/j.chom.2016.06.006.
[14] G. Gay, L. Braun, M.P. Brenier-Pinchart, J. Vollaire, V. Josserand, R.L. Bertini, A. Varesano, B. Touquet, P.J. De Bock, Y. Coute, I. Tardieux, A. Bougdour, M. A. Hakimi, Toxoplasma gondii TgIST co-opts host chromatin repressors dampening STAT1-dependent gene regulation and IFN-γ-mediated host defenses, J. Exp. Med. 213 (2016) 1779–1798, https://doi.org/10.1084/jem.20160340.
[15] E.E. Rosowski, D. Lu, L. Julien, L. Rodda, R.A. Gaiser, K.D.C. Jensen, J.P.J. Saeij, Strain-specific activation of the NF-κB pathway by GRA15, a novel toxoplasma gondii dense granule protein, J. Exp. Med. 208 (2011) 195–212, https://doi.org/10.1084/jem.20100717.
[16] D. Mukhopadhyay, D. Arranz-Solís, J.P.J. Saeij, Toxoplasma GRA15 and GRA24 are important activators of the host innate immune response in the absence of TLR11, PLoS Pathog. 16 (2020) e1006566, https://doi.org/10.1371/journal.ppat.1008586.
[17] F. Ihara, R.M. Fereig, Y. Himori, K. Kameyama, K. Umeda, S. Tanaka, R. Ikeda, M. Yamamoto, Y. Nishikawa, Toxoplasma gondii dense granule proteins 7, 14, and 15 are involved in modification and control of the immune response mediated via NF-κB pathway, Front. Immunol. 11 (2020) 1709, https://doi.org/10.3389/fimmu.2020.01709.
[18] L.O. Sangaré, N. Yang, E.K. Konstantinou, D. Lu, D. Mukhopadhyay, L.H. Young, J. P.J. Saeij, Toxoplasma GRA15 activates the NF-Kb pathway through interactions with TNF receptor-associated factors, MBio 10 (2019) e00808–e00819, https://doi.org/10.1128/mbio.00808-19.
[19] J. Napetschnig, H. Wu, Molecular basis of NF-κB signaling, Annu. Rev. Biophys. 42 (2013) 443–468, https://doi.org/10.1146/annurev-biophys-083012-130338.
[20] T. Kawai, S. Akira, Signaling to NF-κB by toll-like receptors, Trends Mol. Med. 13 (2007) 460–469, https://doi.org/10.1016/j.molmed.2007.09.002.
[21] P. Morgado, D.M. Sudarshana, L. Gov, K.S. Harker, T. Lam, P. Casali, J.P. Boyle, M. B. Lodoen, Type II toxoplasma gondii induction of CD40 on infected macrophages enhances interleukin-12 responses, Infect. Immun. 82 (2014) 4047–4055, https://doi.org/10.1128/IAI.01615-14.
[22] A.L. ten Hoeve, M.E. Rodriguez, M. Säflund, V. Michel, L. Magimel, A. Ripoll, T. Yu, M.-A. Hakimi, J.P.J. Saeij, D.M. Ozata, A. Barragan, Hypermigration of macrophages through the concerted action of GRA effectors on NF-κB/p38 signaling and host chromatin accessibility potentiates *Toxoplasma* dissemination, MBio (2024) e0214024, https://doi.org/10.1128/mbio.02140-24.
[23] J.S. Ma, M. Sasai, J. Ohshima, Y. Lee, H. Bando, K. Takeda, M. Yamamoto, Selective and strain-specific NFAT4 activation by the toxoplasma gondii polymorphic dense granule protein GRA6, J. Exp. Med. 211 (2014) 2013–2032, https://doi.org/10.1084/jem.20131272.
[24] T. Hasan, N. Shimoda, S. Nakamura, B.A. Fox, D.J. Bzik, N. Ushio-Watanabe, Y. Nishikawa, Protective efficacy of recombinant toxoplasma gondii dense granule protein 15 against toxoplasmosis in C57BL/6 mice, Vaccine 42 (2024) 2299–2309, https://doi.org/10.1016/j.vaccine.2024.02.062.
[25] J. Chen, Z.Y. Li, E. Petersen, S.Y. Huang, D.H. Zhou, X.Q. Zhu, DNA vaccination with genes encoding toxoplasma gondii antigens ROP5 and GRA15 induces protective immunity against toxoplasmosis in Kunming mice, Expert Rev. Vaccines 14 (2015) 617–624, https://doi.org/10.1586/14760584.2015.1011133.
[26] Y. Tachibana, E. Hashizaki, M. Sasai, M. Yamamoto, Host genetics highlights IFN-γ-dependent toxoplasma genes encoding secreted and non-secreted virulence factors in in vivo CRISPR screens, Cell Rep. 42 (2023) 112592, https://doi.org/10.1016/j.celrep.2023.112592.
[27] M. Silva, T.H. Nguyen, P. Philbrook, M. Chu, O. Sears, S. Hatfield, R.K. Abbott, G. Kelsoe, M.V. Sitkovsky, Targeted elimination of immunodominant B cells drives the germinal center reaction toward subdominant epitopes, Cell Rep. 21 (2017) 3672–3680, https://doi.org/10.1016/j.celrep.2017.12.014.
[28] C.L. Swanson, T.J. Wilson, P. Strauch, M. Colonna, R. Pelanda, R.M. Torres, Type I IFN enhances follicular B cell contribution to the T cell-independent antibody response, J. Exp. Med. 207 (2010) 1485–1500, https://doi.org/10.1084/jem.20092695.
[29] M. Okamoto, M. Sasai, A. Kuratani, D. Okuzaki, M. Arai, J.B. Wing, S. Sakaguchi, M. Yamamoto, A genetic method specifically delineates Th1-type Treg cells and their roles in tumor immunity, Cell Rep. 42 (2023) 112813, https://doi.org/10.1016/j.celrep.2023.112813.
[30] H. Lambert, N. Hitziger, I. Dellacasa, M. Svensson, A. Barragan, Induction of dendritic cell migration upon toxoplasma gondii infection potentiates parasite dissemination, Cell. Microbiol. 8 (2006) 1611–1623, https://doi.org/10.1111/j.1462-5822.2006.00735.x.
[31] J. Reyes, G.S. Yap, Macrophage to dendritic cell transitioning induced by toxoplasma, Trends Parasitol. 39 (2023) 10–11, https://doi.org/10.1016/j.pt.2022.11.007.
[32] A.K. Bhandage, G.C. Olivera, S. Kanatani, E. Thompson, K. Loré, M. Varas-Godoy, A. Barragan, A motogenic gabaergic system of mononuclear phagocytes facilitates

dissemination of coccidian parasites, Elife 9 (2020) e60528, https://doi.org/10.7554/eLife.60528.
[33] C. Young, R. Brink, The unique biology of germinal center B cells, Immunity 54 (2021) 1652–1664.
[34] E.C. Ross, A.L. ten Hoeve, J.P.J. Saeij, A. Barragan, Toxoplasma effector-induced ICAM-1 expression by infected dendritic cells potentiates transmigration across polarised endothelium, Front. Immunol. 13 (2022) 950914, https://doi.org/10.3389/fimmu.2022.950914.
[35] A. Sapoznikov, S. Kozlovski, N. Levi, S.W. Feigelson, O. Regev, N. Davidzohn, S. Ben-Dor, R. Haffner-Krausz, E. Feldmesser, N. Wigoda, E. Petrovich-Kopitman, M. Biton, R. Alon, Dendritic cell ICAM-1 strengthens synapses with CD8 T cells but is not required for their early differentiation, Cell Rep. 42 (2023) 112864, https://doi.org/10.1016/j.celrep.2023.112864.
[36] A. Scholer, S. Hugues, A. Boissonnas, L. Fetler, S. Amigorena, Intercellular adhesion molecule-1-dependent stable interactions between T cells and dendritic cells determine CD8+ T cell memory, Immunity 28 (2008) 258–270, https://doi.org/10.1016/j.immuni.2007.12.016.
[37] K.D.C. Jensen, K. Hu, R.J. Whitmarsh, M.A. Hassan, L. Julien, D. Lu, L. Chen, C. A. Hunter, J.P.J. Saeij, Toxoplasma gondii rhoptry 16 kinase promotes host resistance to oral infection and intestinal inflammation only in the context of the dense granule protein gra15, Infect. Immun. 81 (2013) 2156–2167, https://doi.org/10.1128/IAI.01185-12.
[38] G.D. Eom, K.B. Chu, H.J. Kang, M.J. Kim, K.W. Yoon, J. Mao, S.H. Lee, M. A. Ahmed, E.K. Moon, F.S. Quan, Protective mucosal and systemic immunity induced by virus-like particles expressing toxoplasma gondii cyst wall protein, PLoS One 18 (2023) e0283928, https://doi.org/10.1371/journal.pone.0283928.
[39] E.F. Merritt, J.A. Kochanowsky, P. Hervé, A.A. Watson, A.A. Koshy, Toxoplasma type II effector GRA15 has limited influence in vivo, PLoS One 19 (2024) e0300764, https://doi.org/10.1371/journal.pone.0300764.
[40] K. Araki, B. Youngblood, R. Ahmed, Programmed cell death 1-directed immunotherapy for enhancing T-cell function, Cold Spring Harb. Symp. Quant. Biol. 78 (2013) 239–247, https://doi.org/10.1101/sqb.78.019869.
[41] A.E. Griep, R. Herber, S. Jeon, J.K. Lohse, R.R. Dubielzig, P.F. Lambert, Tumorigenicity by human papillomavirus type 16 E6 and E7 in transgenic mice correlates with alterations in epithelial cell growth and differentiation, J. Virol. 67 (1993) 1373–1384. https://journals.asm.org/journal/jvi.
[42] N. Ohnishi, H. Yuasa, S. Tanaka, H. Sawa, M. Miura, A. Matsui, H. Higashi, M. Musashi, K. Iwabuchi, M. Suzuki, G. Yamada, T. Azuma, M. Hatakeyama, Transgenic expression of *Helicobacter pylori* CagA induces gastrointestinal and hematopoietic neoplasms in mouse, Proc. Natl. Acad. Sci. USA 105 (2008) 1003–1008. www.pnas.org/cgi/content/full/.
[43] Q. Liu, W.W. Gao, H.M. Elsheikha, J.J. He, F.C. Li, W. Bin Yang, X.Q. Zhu, Transcriptomic analysis reveals toxoplasma gondii strain-specific differences in host cell response to dense granule protein GRA15, Parasitol. Res. 117 (2018) 2785–2793, https://doi.org/10.1007/s00436-018-5966-8.
[44] P. Wang, S. Li, Y. Zhao, B. Zhang, Y. Li, S. Liu, H. Du, L. Cao, M. Ou, X. Ye, P. Li, X. Gao, P. Wang, C. Jing, F. Shao, G. Yang, F. You, The GRA15 protein from toxoplasma gondii enhances host defense responses by activating the interferon stimulator STING, J. Biol. Chem. 294 (2019) 16494–16508, https://doi.org/10.1074/jbc.RA119.009172.
[45] K.B. Chu, F.S. Quan, Advances in toxoplasma gondii vaccines: current strategies and challenges for vaccine development, Vaccines (Basel) 9 (2021) 413, https://doi.org/10.3390/vaccines9050413.
[46] J. Yang, C. Yang, J. Qian, F. Li, J. Zhao, R. Fang, Toxoplasma gondii α-amylase deletion mutant is a promising vaccine against acute and chronic toxoplasmosis, Microb. Biotechnol. 13 (2020) 2057–2069, https://doi.org/10.1111/1751-7915.13668.
[47] L. Wang, D. Tang, C. Yang, J. Yang, R. Fang, Toxoplasma gondii ADSL knockout provides excellent immune protection against a variety of strains, Vaccines (Basel) 8 (2020) 16, https://doi.org/10.3390/vaccines8010016.